Translational Oncology
www.transonc.com

Volume 3 Number 2 April 2010 pp. 123–134 123

Transferrin Receptor 2 Is Frequently and Highly Expressed in Glioblastomas

Alessia Calzolari*, Luigi Maria Larocca†, Silvia Deaglio‡, Veronica Finisguerra*, Alessandra Boe*, Carla Raggi*, Lucia Ricci-Vitani*, Francesco Pierconti§, Fabio Malavasi‡, Ruggero De Maria*, Ugo Testa* and Roberto Pallini§

*Department of Hematology, Oncology and Molecular Medicine, Istituto Superiore di Sanità, Rome, Italy; †Institute of Human Pathology, Catholic University School of Medicine, Rome, Italy; ‡Department of Genetics, Biology and Biochemistry & CeRMS, University of Torino Medical School, Turin, Italy; §Department of Neurosurgery, Catholic University, Rome, Italy

Abstract

Under physiological conditions, transferrin receptor 2 (TfR2) is expressed in the liver and its balance is related to the cell cycle rather than to intracellular iron levels. We recently showed that TfR2 is highly expressed in glioblastoma cell lines. Here, we demonstrate that, in these cells, TfR2 appears to localize in lipid rafts, induces extracellular signal–regulated kinase 1/2 phosphorylation after transferrin binding, and contributes to cell proliferation, as shown by RNA silencing experiments. *In vitro* hypoxic conditions induce a significant TfR2 up-regulation, suggesting a role in tumor angiogenesis. As assessed by immunohistochemistry, the level of TfR2 expression in astrocytic tumors is related to histologic grade, with the highest expression observed in glioblastomas. The level of TfR2 expression represents a favorable prognostic factor, which is associated with the higher sensitivity to temozolomide of TfR2-positive tumor cells *in vitro*. The endothelial cells of glioblastoma vasculature also stain for TfR2, whereas those of the normal brain vessels do not. Importantly, TfR2 is expressed by the subpopulation of glioblastoma cells with properties of cancer-initiating cells. TfR2-positive glioblastoma cells retain their TfR2 expression on xenografting in immunodeficient mice. In conclusion, our observations demonstrate that TfR2 is a neoantigen for astrocytomas that seems attractive for developing target therapies.

Translational Oncology (2010) 3, 123–134

Introduction

Cellular iron uptake is mediated by a ubiquitously expressed receptor for transferrin (Tf), called transferrin receptor 1 (TfR1) [1]. TfR1 plays a key role in the control of the rate of cellular iron uptake, tuning the amount of iron delivered to the cells to the metabolic needs.

In 1999, Kawabata et al. [2] cloned a second TfR-like molecule known as the transferrin receptor 2 (TfR2). Differently from TfR1, TfR2 is not regulated by intracellular iron levels and it seems to be regulated in accordance with the cell cycle [3,4]. Major differences between TfR1 and TfR2 concern their expression patterns. TfR1 is expressed on all cells, except mature erythrocytes and terminally differentiated cells, whereas human TfR2 messenger RNA (mRNA) is highly expressed in the liver and, to a lesser extent, in erythroid cells, spleen, lung, muscle, prostate, and peripheral mononuclear cells [2,3]. Furthermore, mutations of the TfR2 gene produce hemochromatosis type 3, with significant hepatic iron loading [5,6], and TfR2-deficient mice show a phenotype of parenchymal iron overload and features of human TfR2-related hemochromatosis [6]. These observations clearly indicate that TfR2 has a unique, yet unknown role in the regulation of iron homeostasis rather than a simple contribution to cellular iron uptake. This conclusion is reinforced by a recent study showing that TfR2, at variance with TfR1, is localized in lipid rafts, peculiar cell membrane domains involved in the generation of receptor-mediated cell signaling [7]. In a recent study, we explored TfR2 expression in a panel of cancer cell lines, including glioblastomas (GBMs), and we observed that approximately 40% of these cell lines express TfR2 [8].

Address all correspondence to: Dr. Ugo Testa, Department of Hematology, Oncology and Molecular Medicine, Istituto Superiore di Sanità, Viale Regina Elena 299, 00161 Rome, Italy. E-mail: ugo.testa@iss.it
Received 15 September 2009; Revised 15 September 2009; Accepted 11 November 2009

Copyright © 2010 Neoplasia Press, Inc. All rights reserved 1944-7124/10/$25.00
DOI 10.1539/tlo.09274

GBM is the most malignant and, unfortunately, the most common brain tumor: its incidence is approximately 5 cases per 100,000 people [9]. Although molecular markers for GBM have helped identify patients responsive to current therapies [10], the overall survival of responsive patients has not substantially changed in the last 20 years [11].

The expression of TfR1 has been explored in normal brain and in brain tumors. In normal brain, TfR1 was detected primarily in endothelial cells. Among brain tumors, astrocytomas clearly express TfR1, with GBM showing the highest expression [12]. As in other neoplasms, TfR1 in gliomas induces increased intracellular iron accumulation [13] and promotes tumor progression by two mechanisms, namely an increase in proliferation rate and glutamate production [14], the latter mechanism providing space for the progressing tumor mass [15]. Accordingly, it was suggested that TfR1 might be an appropriate target for ligand-directed brain tumor immunotherapy. To this purpose, Tf-toxin (*Pseudomonas* exotoxin A or diphtheria toxin mutant CRM107) conjugates were constructed and a strong cytotoxic effect on GBM cells was demonstrated *in vitro* [16]. Regional therapy for recurrent malignant brain tumors with Tf-CRM107 conjugate has also been tested in a small series of GBM patients by interstitial microinfusion with encouraging results [16]. In a phase 2 trial, Tf-CRM107 resulted in a 35% response rate [17]. However, curative doses induced peritumoral brain toxicity, consisting of thrombosed cortical vessels, which were explained by the presence of TfR1 on endothelial cells.

In the present study, we first explored TfR2 expression in human GBM cell lines and found that TfR2 appears to localize in lipid rafts and that its activation, after binding with Tf, induces extracellular signal–regulated kinase 1/2 (ERK 1/2) phosphorylation. TfR2 silencing reduces GBM cell proliferation. Then, we assessed TfR2 expression in human astrocytomas of various histologic grades. Interestingly, we found that TfR2 is frequently and highly expressed in anaplastic astrocytomas (AA) and in GBM, with absent or very weak expression on the endothelial cells of normal brain. Furthermore, we show that TfR2-positive GBM cell lines, including one GBM stem cell line, maintain TfR2 expression on xenografting in immunodeficient mice. These results candidate TfR2 for target therapies of GBM tumors.

Materials and Methods

Antibodies

Anti-TfR2 monoclonal antibodies (mAbs, clones G/14C2 and G/14E8) have been described in a previous study [18]. Anti-human TfR1 used for Western blot analysis was from Zymed Laboratories (South San Francisco, CA). Fluorescein isothiocyanate–conjugated antihuman TfR1 used for flow cytometry analysis was from Becton Dickinson (San Jose, CA). Anti–caveolin-1 (N-20) was obtained from Santa Cruz Biotechnology (Santa Cruz, CA). Anti–phospho-ERK1/ERK2 (T202/Y204), anti–human/mouse/rat ERK1/ERK2, and anti–human/mouse/rat hypoxia-inducible factor 1α (HIF-1α) were from R&D Systems (Minneapolis, MN).

Cell Lines

Human GBM cell lines TB10, U87MG, T98G, and U251 were grown in Dulbecco's modified Eagle medium (DMEM; Gibco, Invitrogen, Milan, Italy) containing 10% fetal calf serum (Euroclone, Milan, Italy). The human GBM stem cell lines BTSC1 and BTSC83 were also used (these cell lines were coded as 1 and 7, respectively, in Ricci-Vitiani et al. [19]).

Cell Treatments

To mimic hypoxia, GBM cell lines were incubated for either 24 or 48 hours in the presence of $CoCl_2$ (100 μM; Sigma Co, St Louis, MO) or under reduced oxygen tension (5% and 1% O_2) and then analyzed for TfR1 and TfR2 expression. In other experiments, GBM cells were incubated in the presence of the MEK1 inhibitor PD184352 (Calbiochem, San Diego, CA) added at the final concentrations of either 1 or 2 μM.

In some experiments, GBM cell lines have been incubated with temozolomide (from 25 to 300 μM) and then, at various days after drug addition, analyzed for the number of living cells and the cell cycle status.

In stimulation experiments, serum-starved GBM cells lines have been treated for various times with DMEM containing 30 μM holo-Tf.

Flow Cytometry Analysis

Aliquots of nonadherent cells were harvested from the flask cultures and processed as reported later. Adherent cells were detached from the tissue culture flasks using a nonenzymatic detaching solution (Sigma). Cell aliquots were washed twice in cold PBS and then incubated in the presence of 1 μg/ml anti-TfR2 mAb (G/14E8) or 1 μg/ml irrelevant mouse immunoglobulin G (IgG) for 30 minutes at 4°C, washed twice in cold PBS, and then incubated with affinity-purified phycoerythrin-labeled goat antimouse IgGs diluted 1:40 (Dakopatts, Copenhagen, Denmark). After two additional washes in PBS, the cells were analyzed in a FACS Scan flow cytometer (Becton Dickinson). For TfR1 labeling, the cells were incubated with phycoerythrin-conjugated anti-TfR1 Ab (Becton Dickinson).

Western Blot Analysis

Cellular lysates were resolved by 7.5% SDS-PAGE under reducing and denaturing conditions and transferred to nitrocellulose filter. The blots were blocked using 5% nonfat dry milk in TBST (10 mM Tris-HCl pH 8.0, 150 mM NaCl, 0.1% Tween 20) for 1 hour at room temperature, followed by incubation with primary antibodies. After washing with TBST, the filters were incubated with appropriate horseradish peroxidase–conjugated secondary antibodies (Bio-Rad, Hercules, CA) for 1 hour at room temperature. Immunoreactivity was revealed by using an ECL detection kit (Pierce, Rockford, IL).

Cell Cycle Analysis by Propidium Iodide/Fluorescence-Activated Cell Sorting

Cells were harvested, washed, fixed, and resuspended in 400 μl of propidium iodide solution (50 μg/ml propidium iodide, 0.1% Triton X-100, and 0.1% sodium citrate in PBS; Cycle Plus DNA Staining Kit; Becton Dickinson). The cells were then analyzed by flow cytometry using a software dedicated for DNA analysis (ModFit LT Software; Verity Software House, Topsham, ME).

Confocal Microscopy Analysis

TB10 and U251 cells were plated on coverslips and left to adhere overnight. Coverslips were stained with mouse mAbs directed against TfR2 (15 minutes at 37°C), followed by a Texas Red–conjugated goat antimouse IgG (Jackson Immunoresearch, West Grove, PA). Cells were then fixed and permeabilized (4% paraformaldehyde/2% sucrose, 10 minutes at room temperature, plus 0.1% saponin, 30 minutes at room temperature), saturated (1% normal goat serum), and stained with a rabbit polyclonal anti–caveolin-1 (BD Bioscience, Bedford, MA), followed by an Alexa 488–conjugated antirabbit IgG (Jackson Immunoresearch). All images were acquired using an Olympus 1x70 (FV300 System) confocal microscope and processed with the Analysis software (Olympus Life Sciences, Milan, Italy).

Knockdown of TfR2 Using Small Interfering RNA

TfR2$^+$ cells at 30% to 50% confluency were transfected overnight with 20, 40, or 60 nM human TfR2 SMART pool (Dharmacon, Lafayette, CO) or Stealth-negative control small interfering RNA (siRNA; Invitrogen) using Oligofectamine (Invitrogen). After transfection, the medium was replaced with DMEM containing 5% fetal calf serum and incubated for a further 48 hours before assay. Levels of TfR2 protein were determined by flow cytometry and Western blot analysis. Statistical differences in TfR2 expression were determined using one-way analysis of variance and Bonferroni tests.

In some experiments, after transfection with control siRNA (40 nM) or TfR2 siRNA (60 nM), U251 cells were treated for 72 hours with temozolomide 300 μM and analyzed for the number of living cells and the cell cycle status.

Isolation of Caveolae-Enriched Membrane Fractions

Caveolae-enriched membrane fractions were isolated according to standard protocols [20,21]. Briefly, cell pellet was dissolved in 0.75 ml of 2(*N*-morpholino)ethanesulfonic acid-buffered saline (25 mM 2(*N*-morpholino)ethanesulfonic acid/pH 6.5, 150 mM NaCl) containing 1% Triton X-100 at 4°C. Cell lysate was Dounce-homogenized, adjusted to 40% sucrose, and placed at the bottom of an ultracentrifuge tube. A 5% to 30% linear sucrose gradient was then placed above the homogenate, and the mixture was centrifuged at 45,000 rpm for 16 hours at 4°C in a SW60 rotor (Beckman Instruments, Palo Alto, CA). The caveolar fractions are visible as a light scattering band migrating at approximately 20% sucrose. Twelve 0.375-ml fractions were collected from the top to the bottom of the gradient, separated by SDS-PAGE and subjected to immunoblot analysis. Fractions 1 and 2 generally do not contain proteins, and thus, they were not subjected to SDS-PAGE. Fraction 12 represents the nuclear portion.

Patients and Tumor Tissue Samples

This study included 81 adult patients who underwent craniotomy for tumor resection at the Institute of Neurosurgery, Catholic University School of Medicine, Rome, Italy, and were confirmed to have low-grade astrocytoma (LGA; 24 patients), AA (22 patients), and GBM (35 patients) in the supratentorial compartment. Patients of pediatric age were not included. All the patients provided written informed consent according to research proposals approved by the ethical committee of the Catholic University School of Medicine.

Brain tissue samples, which were adjacent to the tumor that had been resected by radical excision, were also studied. Tumors located in the optic nerve, hypothalamus, thalamus, suprasellar region, or posterior fossa were excluded. There were 47 male and 34 female patients. The age of the patients ranged from 22 to 76 years; the mean age at surgery was 47.5 years. No patient had received radiation therapy before surgery. The tumors were diagnosed according to the classification of Burger and Scheithauer [22].

The postsurgical treatment plan included radiotherapy to limited fields (2 Gy per fraction, once a day, 5 days a week, 60 Gy total dose) and concomitant temozolamide (75 mg/m^2 of body surface area per day) for 7 days a week from the first to the last day of radiotherapy, followed by five cycles of adjuvant temozolamide (at 200 mg/m^2 of body surface area o days 1 to 5) given at 4-week intervals. Survival was calculated from the date of diagnosis.

Immunohistochemistry for TfR2

The anti-TfR2 mouse monoclonal antibody (1:150; clone G/14C2) was used. The antigen was retrieved by microwave oven processing (two cycles of 5 minutes, 500 W) in citrate buffer and the bound antibody was visualized with the avidin-biotin complex peroxidase method (ABC ELITE Detection System; Vector, Burlingame, CA). Hydrogen peroxide, normal goat blocking serum, biotinylated immunoglobulins, avidin-biotin complexes, and 3-amino-9-ethyl-ethylcarbazole substrate solutions were used according to the manufacturer. Sections were lightly counterstained with hematoxylin for 25 seconds and mounted in Permount Slide Mounting Fluid (The Science Co, Denver, CO). The intensity of staining for TfR2 in the tumor tissue sections was graded on a scale from 0 to 3+, with 0 indicating no detectable staining, 1+ slight staining of the cytoplasm only discernible in 400× high-power field, 2+ moderate staining of the cytoplasm outlining the cellular details clearly detectable in 100× to 200× field, and 3+ intense staining of all the cytoplasm that obscures the nucleus detectable in 20× field. The percentage of TfR2-positive cells was determined with respect to the total number of cells in high-power fields (400×). In each case, more than 1500 cells were counted in randomly selected nonsuperimposing areas of the tumor, which were devoid of massive necrosis. The percentage of TfR2-positive cells was evaluated independently by two observers (F.P. and L.M.L.) who were unaware of the clinical data. Differences between the extreme counts of the two observers never exceeded 5%. Interobserver agreement was reached in the first analysis in 90% of cases; for the remaining cases, a consensus was reached by a joint review of the slides.

Tumor Xenografts in Immunodeficient Mice

Four-week-old male nude mice (Harlan, Udine, Italy) were used as hosts for the *in vivo* model. The experiments on animals were approved by the ethical committee of the Catholic University School of Medicine, Rome, Italy. For subcutaneous grafting, either 1×10^6 TB10 GBM cells [23] or 5×10^5 BTSC83 GBM stem cells [19,24] were harvested, washed twice, and resuspended in cold PBS. Then, 100 μl of cells were mixed with 100 μl of Matrigel (BD Bioscience) on ice, and the mixture was implanted by subcutaneous injection using a 25-gauge needle. Only one injection was performed on a single mouse. After grafting, mice were kept under pathogen-free conditions in positive-pressure cabinets (Tecniplast Gazzada, Varese, Italy) and observed weekly for appearance of subcutaneous nodules at injection site. Mice were killed with an overdose of barbiturate either 12 weeks after injection or when the subcutaneous nodules reached 15 mm in maximum diameter. The subcutaneous tumor was removed, fixed in 4% paraformaldehyde, embedded into paraffin, cut in 5-μm-thick sections, and stained with hematoxylin and eosin. Immunohistochemical analysis was performed as above.

Statistical Methods

Differences in TfR2 expression among LGA, AA, and GBM groups were evaluated using the χ^2 test. In GBM tumors, the relationship between the level of TfR2 staining and overall patients' survival was evaluated by using Pearson's correlation coefficient. The coefficient was analyzed by a t test. Statistical significance was assigned to $P < .05$. The computer software used for statistical analysis was Fig. P (Biosoft, Cambridge, UK).

Results

TfR2 Expression in GBM Cell Lines

We investigated TfR2 expression in four GBM cell lines (TB10, U87MG, T98G, and U251), showing that TB10 and U251 strongly express TfR2, as assessed both by flow cytometry and by Western blot

analysis (Figure 1, *A* and *B*). Interestingly, the TB10 GBM cell line expresses TfR2 but not TfR1 (CD71; Figure 1, *A* and *B*).

We also evaluated TfR2 expression in two human GBM stem cell lines (BTSC1 and BTSC83), which have been established in our laboratory from dissociation of tumor spheres under stem cell culturing conditions [19,24]. The experiment showed that TfR2 is highly expressed in BTSC83 cell line (Figure 1, *A* and *B*).

TfR2 Localization in Lipid Rafts

In a previous study, we showed that TfR2 is localized in lipid rafts in erythroleukemic K562 and hepatoma HepG2 cells [7]. Therefore, it seemed important to evaluate TfR2 localization in GBM cells. A sucrose density gradient ultracentrifugation of cell lysates was used to purify lipid raft microdomains. After sucrose gradient centrifugation, detergent-resistant lipid rafts float to low-density fractions because of their high lipid content. These insoluble membranes, visible as a white opalescent band in fraction numbers 4, 5, 6, and 7, were compared with soluble fraction numbers 8, 9, 10, and 11 for TfR2 content. Immunoblot analysis performed on SDS-PAGE loaded with equal amount of protein for each fraction showed that TfR2 was predominantly located in insoluble fractions in both TB10 and U251 cells. Caveolin-1, which was used to track the position of caveolae-enriched membranes, was detected in insoluble fractions (Figure 1, *C* and *D*). As expected, in U251 cells, the nonraft marker TfR1 was localized in soluble fractions 9 to 11 (Figure 1*D*).

To confirm the immunoblot data concerning the plasma membrane sublocation of TfR2, we performed immunofluorescence double staining to localize TfR2 and the raft-resident cav-1 protein. In both TB10 and U251 cells, TfR2 and cav-1 largely colocalized in the plasma membrane (Figure 2).

TfR2 Activates ERK1/ERK2 Phosphorylation

Given that sucrose gradient centrifugation experiments provided some evidence that TfR2 was localized at the level of lipids rafts and that these microdomains play an important role in signal transduction [25], it seemed logical to evaluate whether triggering this receptor may activate signal transduction. Because mitogen-activated protein kinase (MAPK) activation was proved to be crucial in signal transduction of a large number of membrane receptors and ERK1/ERK2 have been shown to be phosphorylated after TfR2 activation in K562 cells [7], we investigated whether TfR2 stimulation might lead to the activation of this pathway in GBM cells. To address this point, we performed stimulation of serum-starved TB10 or U251 cells with human Tf. The results of this experiment showed that exposure of TB10 cells in the presence holo-Tf 30 μM resulted in a marked phosphorylation of ERK1/ERK2 (Figure 3*A*). Because TB10 cells possess only TfR2 and completely lack TfR1, the stimulatory effect of holo-Tf on ERK1/ERK2 phosphorylation could be related only to TfR2 activation. In parallel, we showed that TfR2 cross-linking with the anti-TfR2 mAb G/14C2 (data not shown) and treatment with apo-Tf (Figure 3*A*) led to ERK1/ERK2 activation. To further demonstrate that the stimulatory effect of holo-Tf is related to TfR2 and not to TfR1, serum-starved TfR2$^-$ U87MG cells have been treated for the indicated times with holo-Tf 30 μM, showing no phosphorylation of ERK1/ERK2 (Figure 3*A*).

In parallel, we have evaluated the capacity of specific MEK1 inhibitors, such as PD184352, to inhibit the growth of TB10 cells. This experiment showed that PD184352 potently inhibited in a dose-dependent manner

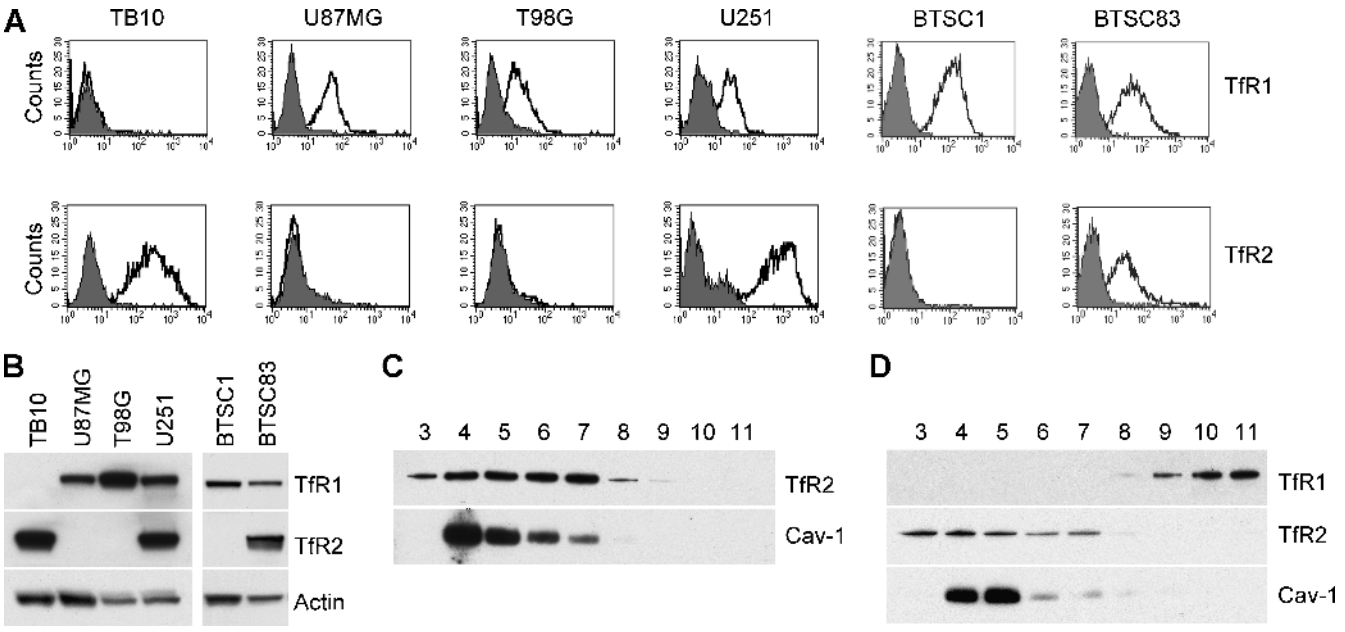

Figure 1. TfR2 expression in GBM cell lines. (A) Flow cytometry analysis of TfR1 and TfR2 expression in TB10, U87MG, T89G, and U251 GBM cell lines and in BTSC1 and BTSC83 GBM stem cell lines. Cells have been labeled with anti-TfR1 and anti-TfR2 mAbs and then analyzed by flow cytometry. (B) Western blot analysis of TfR1 and TfR2 expression in TB10, U87GM, T98G, and U251 GBM cell lines and in BTSC1 and BTSC83 GBM stem cell lines. Blots were stripped and reprobed for actin to ensure equivalent loading and transfer. (C and D) Association of TfR2 with lipid rafts/caveolae by density gradient centrifugation. TB10 (C) and U251 (D) cells were lysed in Triton X-100 and subjected to sucrose gradient centrifugation. Aliquots of fractions collected from the top of the gradient were analyzed by Western blot analysis with the use of antibodies against TfR1, TfR2, and caveolin-1 (Cav-1). Equal protein amounts for each fraction were loaded on SDS-PAGE.

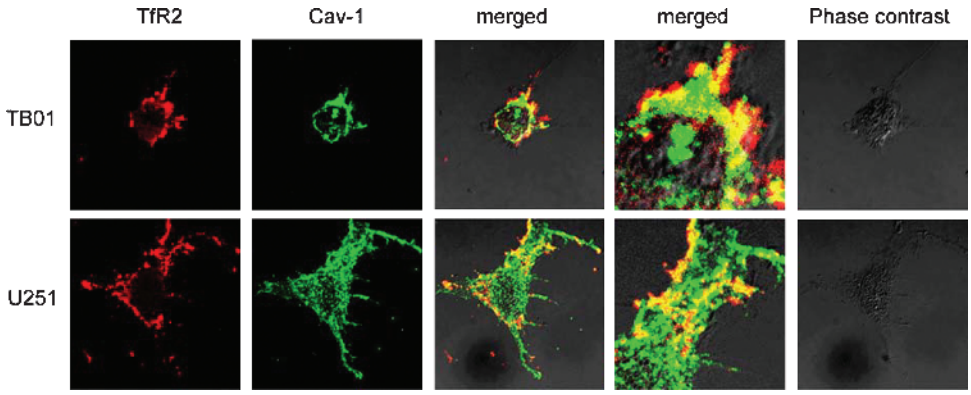

Figure 2. Association between TfR2 and caveolin-1 in lipid rafts as shown by immunofluorescence experiments. TB10 and U251 cells were plated on glass coverslips and left to adhere overnight. TfR-2 was visualized by incubating cells with anti–TfR_2 mAb and then with Texas Red–conjugated antimouse IgG (red fluorescence). Cells were then fixed, permeabilized, and then labeled with caveolin-1 antibody followed by Alexa 488–conjugated antirabbit antibody (green fluorescence). An image of a representative cells is shown reporting the red (TfR-2), green (Cav-1), merged fluorescence (at two different magnifications), and phase contrast.

the growth of TB10 cells (Figure 3*B*). Similar results have been obtained in TfR2$^-$ GBM cells (data not shown), suggesting that the MAPK pathway contributes to cellular proliferation of GBM cells, regardless of TfR2 expression.

Hypoxia Upmodulates TfR2 Expression

Previous studies have shown that hypoxia is an important modulator of TfR1 expression [26,27]. Conversely, hypoxia regulates the neoangiogenetic mechanisms that are particularly active in GBM [28]. Therefore, it seemed important to evaluate a possible effect of hypoxia on TfR2 modulation in GBM cell lines. To this end, we grew TB10 and U251 cells in the presence of 100 μM $CoCl_2$, an agent mimicking hypoxia, or under reduced oxygen tension (5% and 1% O_2) and we measured the level of TfR2 expression both by flow cytometry and by Western blot analysis. As expected, $CoCl_2$ treatment and low oxygen tension (1% O_2) induced a marked rise of HIF-1α levels (Figure 4*B*). Then, $CoCl_2$ treatment elicited a significant TfR2 upmodulation that was quite remarkable in TB10 cells (Figure 4, *A*, *B*, and *D*). Similarly, TfR2 expression was upmodulated under hypoxic conditions, compared with normal oxygen tension (20% O_2), especially in TB10 cells.

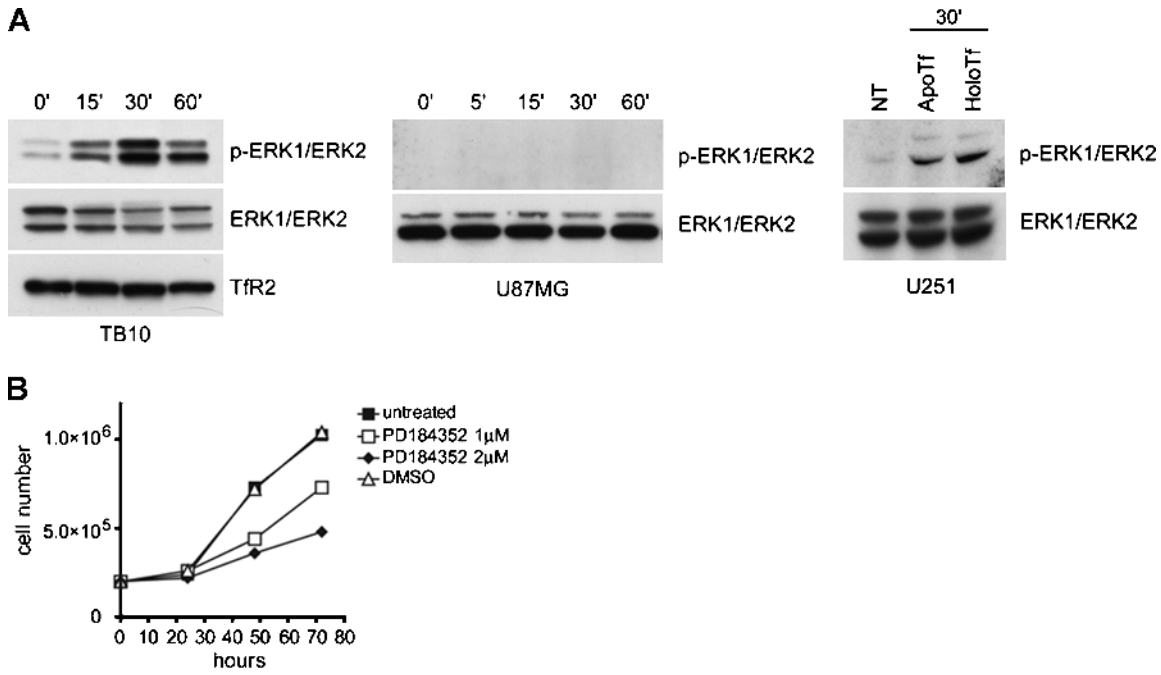

Figure 3. TfR2 stimulation activates ERK1/ERK2 MAPK. (A) Activation of ERK1/ERK2 MAPK. TB10 (left panel) and U87MG (middle panel) cells were serum-starved, treated with 30 μM human holo-Tf for the indicated times and subjected to immunoblot analysis with anti–phospho-ERK1/ERK2. Blots were stripped and reprobed for total ERK1/ERK2 and for TfR2 to ensure equivalent loading and transfer. U251 cells (right panel) were serum-starved, treated with the stimulation medium in the absence (*NT* indicates not treated) or in the presence of 30 μM human holo-Tf and 30 μM human apo-Tf for 30 minutes at 37°C and subjected to immunoblot analysis with anti–phospho-ERK1/ERK2. (B) Effect of ERK1/ERK2 phosphorylation inhibitor on the growth of TB10 cells. TB10 cells have been grown either in the absence or in the presence of the MEK-1 inhibitor PD184352, added either at 1 or 2 μM.

TfR2 Expression in Astrocytic Tumors

Using specific mAbs antihuman TfR2, whose specificity had previously been reported [18], we assessed by immunohistochemistry (IHC) the expression of TfR2 in 81 astrocytic tumors, 24 LGAs (WHO grade 2), 22 AA (WHO grade 3), and 35 GBM (WHO grade 4). The intensity of IHC staining for TfR2 in the tumor cells was graded on a scale ranging from 0 to 3+: 0, no detectable staining; 1+, slight cytoplasmic staining discernible only in a 400× high-power field; 2+, moderate cytoplasmic staining clearly detectable in a 100 to 200× field; and 3+, intense cytoplasmic staining detectable in a 20× field, obscuring cellular details. We also assessed the percentage of TfR2-positive cells relative to the total number of tumor cells.

Results of IHC analysis are presented in Figure 5. Overall, the level of TfR2 expression by the tumor cells was related to histologic grade. Staining for TfR2 was scored 0 to 1+ in 22 (91.7%) of 24 LGA, 6 (27.3%) of 22 AA, and 14 (40%) of 35 GBM tumors (Figure 5*A*). Of 22 cases classified as showing 2+ staining, there were 1 (4.2%) of 24 LGA, 11 (50%) of 22 AA, and 10 (28.6%) of 35 GBM. The highest degree of TfR2 expression (3+) was detected in 1 (4.2%) of 24 LGA, 5 (21.7%) of 22 AA, and 11 (31.4%) of 35 GBM (Figure 5*A*; $P < .05$, χ^2 test). Regarding distribution of TfR2 staining, of 35 GBM, 28 (80%) showed TfR2-positive immunoreaction in more than 50% of the tumor cells, 5 (14.3%) contained 25% to 50% TfR2-positive cells, and 2 (5.7%) had no TfR2-positive cells. Among 22 AA, 2 (9%), 10 (45.5%), 9 (41%), and 1 (4.5%) tumors showed TfR2 expression by more than 50% of cells, by 25% to 50% of cells, by less than 25% of cells, and by 0% of cells, respectively. Finally, of 24 LGA, 2 (8.4%) showed 25% to 50% TfR2-positive cells, 12 (50%) had less than 25% TfR2-positive cells, and 10 (41.6%) were completely devoid of TfR2-positive cells.

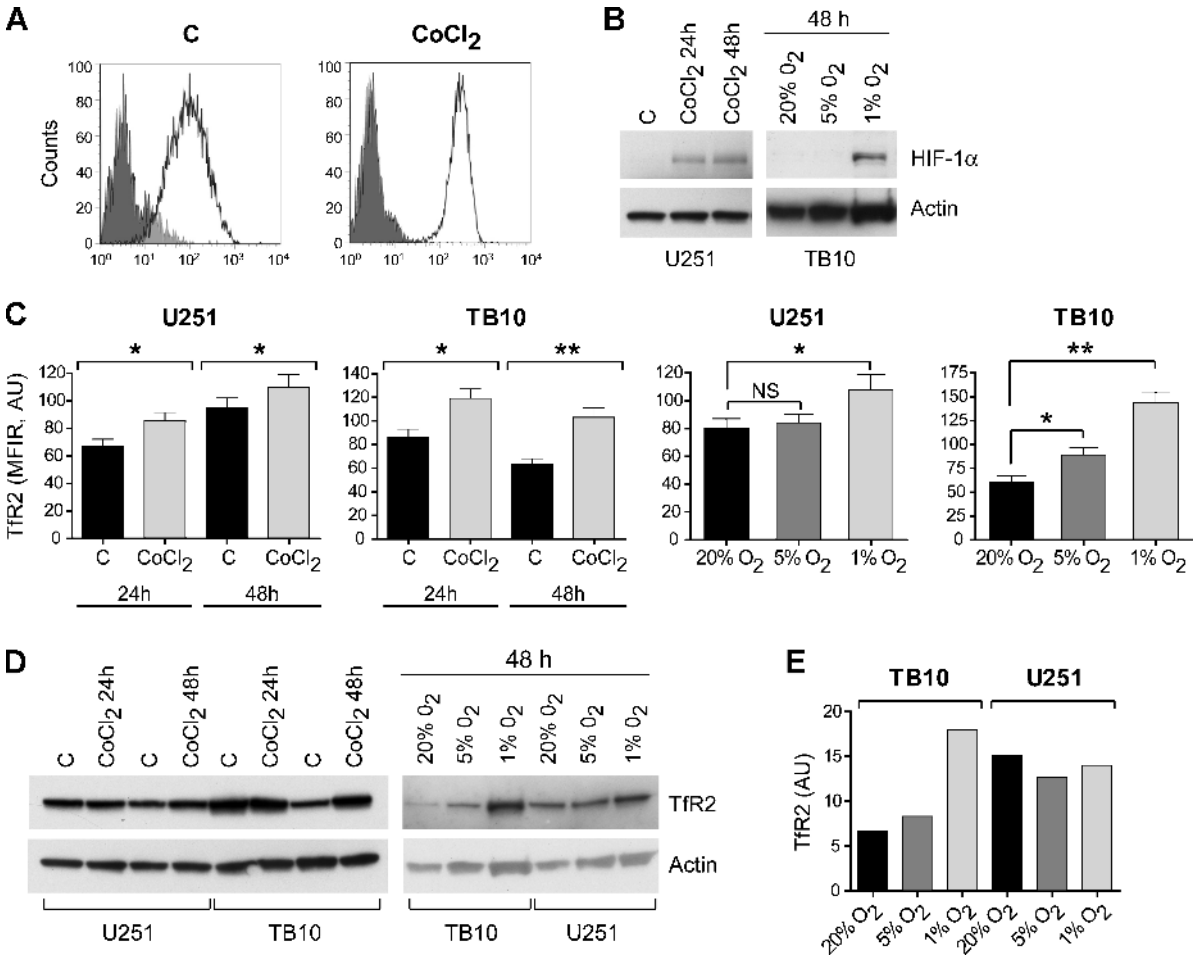

Figure 4. Effect of hypoxia on TfR2 expression. (A) Flow cytometry analysis of TfR2 expression in TB10 cells grown for 40 hours either in the absence (C) or in the presence of 100 μM $CoCl_2$. (B) Western blot analysis of HIF-1α expression in U251 cells grown for either 24 or 48 hours either in the absence (C) or in the presence of 100 μM $CoCl_2$ and in TB10 cells grown for 48 hours under normal (20% O_2) and reduced (5% and 1% O_2) oxygen tension. (C) Analysis of the level of fluorescence (mean fluorescence intensity values normalized with respect to their negative control) of TfR2 labeling observed in TB10 and U251 cells grown for either 24 or 48 hours either in the absence (C) or in the presence of 100 μM $CoCl_2$ or under controlled (20%, 5%, and 1% O_2) oxygen tension. Data represent the mean values ± SEM observed in three independent experiments. *$P < .05$, **$P < .01$. *NS* indicates not significant. (D) Western blot analysis of TfR2 expression in U251 and TB10 cells grown for 24 or 48 hours either in the absence (C) or in the presence of 100 μM $CoCl_2$ or under controlled (20%, 5%, and 1% O_2) oxygen tension. (E) TfR2 levels in TB10 and U251 cells grown under controlled (20%, 5%, and 1% O_2) oxygen tension have been determined by densitometry of Western blot autoradiograms and, after normalization with respect to actin, have been expressed in arbitrary units (AU) and then plotted.

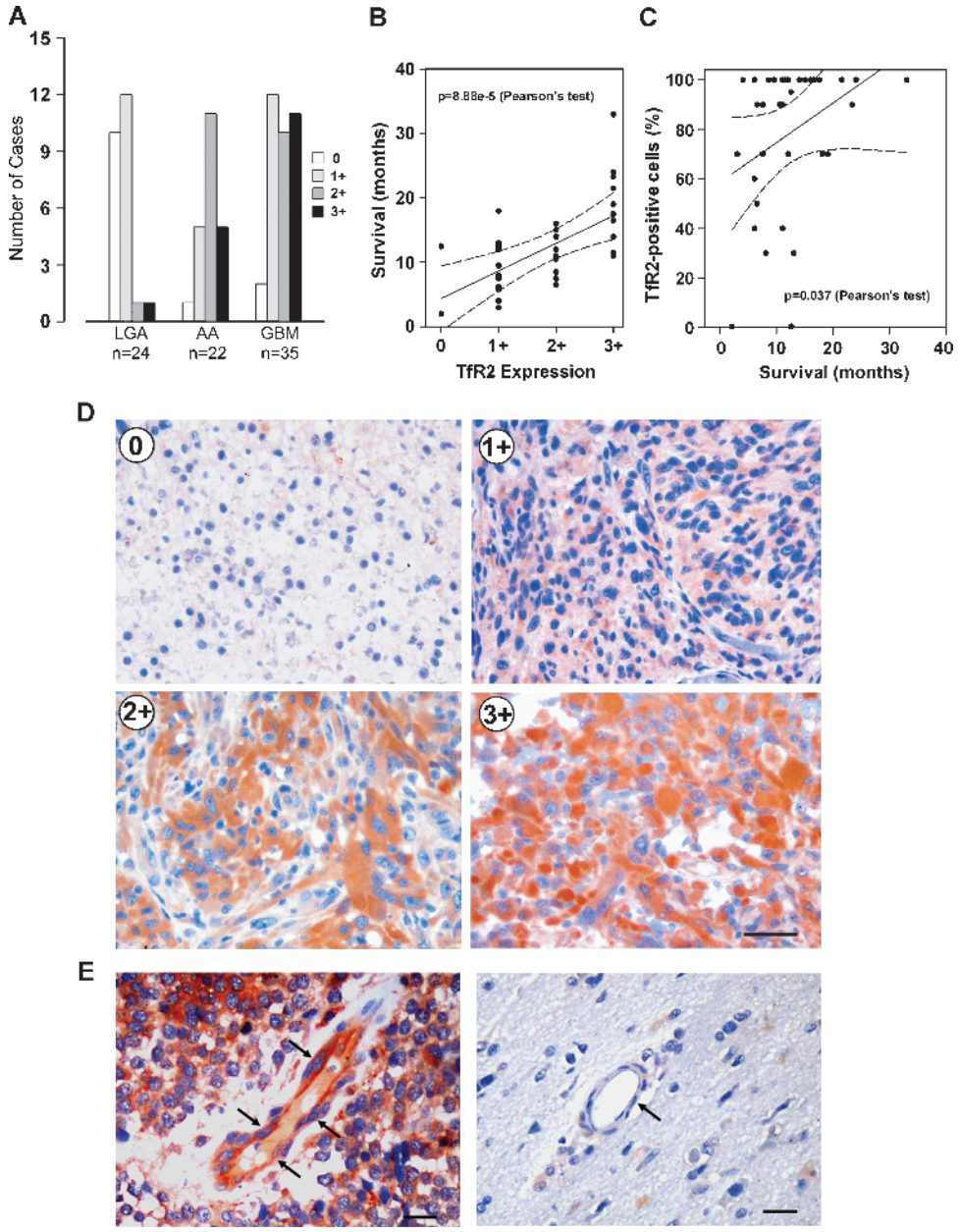

Figure 5. TfR2 expression in astrocytic tumors. (A) Degree of TfR2 expression in 81 astrocytic tumors differing in histologic grade. (B and C) Graphs showing the relationship between overall patients' survival and either the degree of TfR2 immunostaining (B) or the percentage of TfR2-positive cells (C) in 35 GBM tumors. The variables were significantly related with a 95% confidence interval ($P < .0001$ and $P < .05$ in B and C, respectively; Pearson linear correlation coefficient). (D) Immunohistochemical analysis of TfR2-negative (0) LGA, AA scoring 1+ TfR2 expression, GBM showing 2+ TfR2 expression and GBM showing 3+ TfR2 expression. Bar, 75 μm. (E) Anti-TfR2 IHC of blood vessels in a GBM tumor showing immunoreactive endothelial cells (arrows, left panel) and in a normal brain specimen with negative endothelial cells (arrow, right panel). Bar, 35 μm.

In GBM tumors, a highly significant correlation was noted between the expression level of TfR2 and overall patients' survival ($P < .0001$, Pearson linear correlation coefficient), demonstrating that higher levels of TfR2 expression were significantly associated with a better prognosis (Figure 5*B*). A similar relationship, although at a lower level of significance, was also found when the overall patients' survival was plotted against the percentage of TfR2-positive cells in the tumor tissue ($P = .037$, Pearson linear correlation coefficient; Figure 5*C*). Representative examples of TfR2 IHC staining are shown in Figure 5*D*.

It was worthy noting that 21 (60%) of 35 GBM cases scoring 2+ to 3+ showed a prominent staining for TfR2 in the endothelial cells of arterioles and capillaries of the tumor vasculature (Figure 5*E*). In contrast, TfR2 staining was not detected in the vessels of normal brain as well as in the tumor vessels of LGA.

GBM Cell Lines Sensitivity to Temozolomide

Because patients with GBMs expressing higher levels of TfR2 survive longer than patients with low-expressing TfR2 GBMs, it seemed of

interest to compare the *in vitro* sensitivity to temozolomide of $TfR2^+$ and $TfR2^-$ GBM cell lines. To do these experiments, either the $TfR2^+$ TB10 and U251 cell lines or the $TfR2^-$ U87MG and T98G cell lines were grown *in vitro* in the presence of increasing concentrations of temozolomide (from 25 to 300 μM). The results of these experiments were evaluated in terms of the number of living cells and showed that temozolomide exerted a more pronounced inhibitory effect on the growth of $TfR2^+$ than $TfR2^-$ cell lines (Figure 6*A*, *left panel*). The inhibitory effect of temozolomide on GBM cell proliferation was related to a blockade of these cells in G_2/M phase of the cell cycle, and this effect was more pronounced in $TfR2^+$ than in $TfR2^-$ cells (Figure 6*A*, *right panel*).

To investigate whether temozolomide sensitivity of GBM cells was directly related to TfR2 expression in these cells, we have evaluated the effect of TfR2 silencing on temozolomide sensitivity. U251 cells were transfected either with a specific TfR2 siRNA or with a negative control siRNA and then treated for 72 hours with 300 μM temozolomide. The results have shown that TfR2 siRNA treatment of U251 cells does not affect the inhibitory effect of temozolomide on cellular proliferation, as demonstrated by the analysis of the number of living cells (Figure 6*B*, *left panel*) and of the percentage of cells in the G_2/M phase of cell cycle (Figure 6*B*, *right panel*). These experiments clearly demonstrate that the higher sensitivity to temozolomide of $TfR2^+$ cells compared with $TfR2^-$ cells is associated to, but not directly dependent on, TfR2 expression.

TfR2 Silencing Reduces GBM Cell Growth

To evaluate a possible effect of TfR2 on the proliferation of GBM cells, $TfR2^+$ GBM cell lines were transfected either with a specific TfR2 siRNA or with a negative control siRNA. The TfR2 protein was knocked down in TB10 and U251 cells by five- to six-fold (Figure 7, *A* and *B*). There was no significant difference in TfR2 expression between cells transfected with negative control siRNA and those transfected with vehicle alone (Figure 7, *A* and *B*). TfR1 expression was not affected by TfR2 siRNA transfection (Figure 7*A*). Treatment of cells with TfR2 siRNA resulted in significantly reduced cell proliferation, compared with control values (Figure 7*C*). The presence of TfR1 in U251 cells may explain the lower effect of TfR2 silencing on the growth of U251 compared with $TfR1^-$ TB10 cells.

TfR2 Expression in GBM Xenografts

For the *in vivo* experiments, we used two GBM cell lines that had been established in our laboratory [23,24]. The TB10 cell line has been shown both to generate tumor xenografts in nude mice and to express TfR2 under *in vitro* conditions [8,29]. Therefore, this cell line was suited to assess whether TfR2 expression is maintained in *in vivo* conditions. The second GBM cell line (BTSC83), which has been established from dissociation of tumor spheres under stem cell culturing conditions [19,24], would answer the question whether TfR2 is expressed by the subpopulation of GBM cells with properties of cancer initiating cells. IHC revealed that the tumor xenografts generated both by TB10 and by

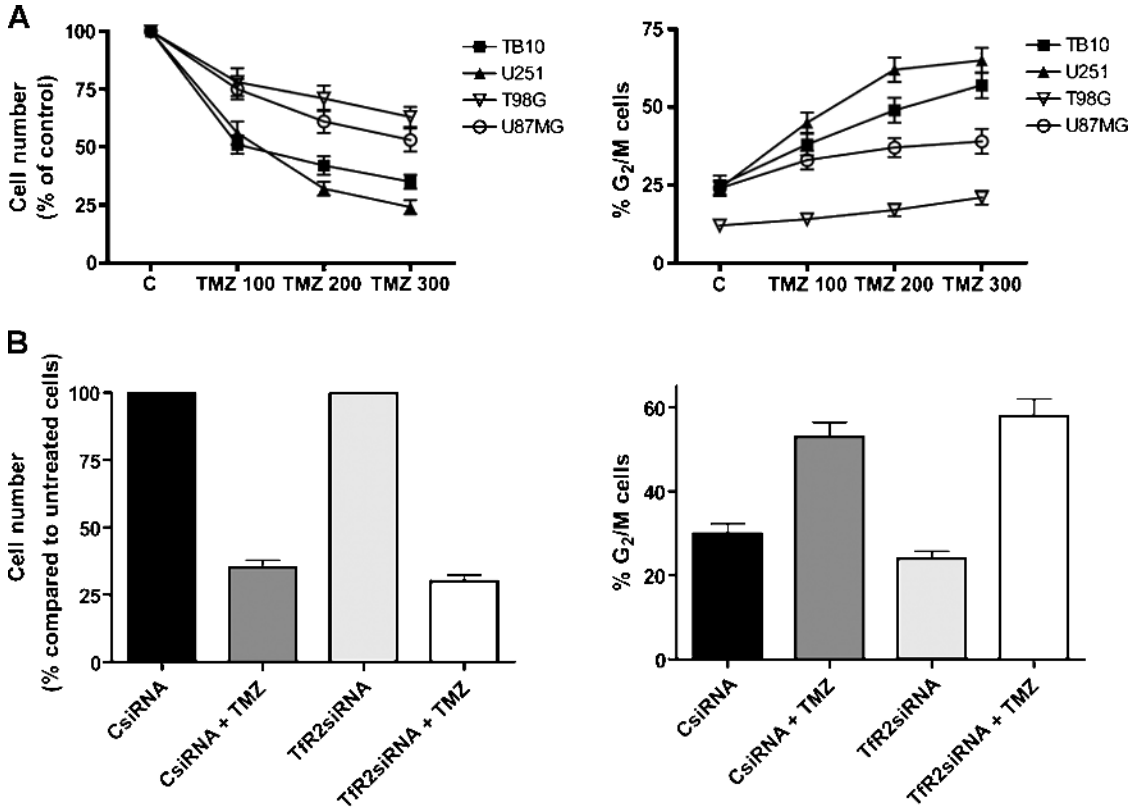

Figure 6. Effect of temozolomide on cell proliferation and cell cycle. (A) Cell lines TB10, U251, T98G, and U87MG were treated with control medium (C) or temozolomide (TMZ) at the indicated concentrations and then trypsinized and counted after 72 hours of incubation at 37°C (left panel). The cells were subjected to cell cycle analysis in flow cytometry. Data shown are percentages of the cells in the G_2/M phase (right panel). (B) U251 cells were transfected with control siRNA (40 nM) or TfR2 siRNA (60 nM), treated for 72 hours with temozolomide 300 μM, and then analyzed for the number of living cells (left panel) and the percentage of the cells in G_2/M phase (right panel).

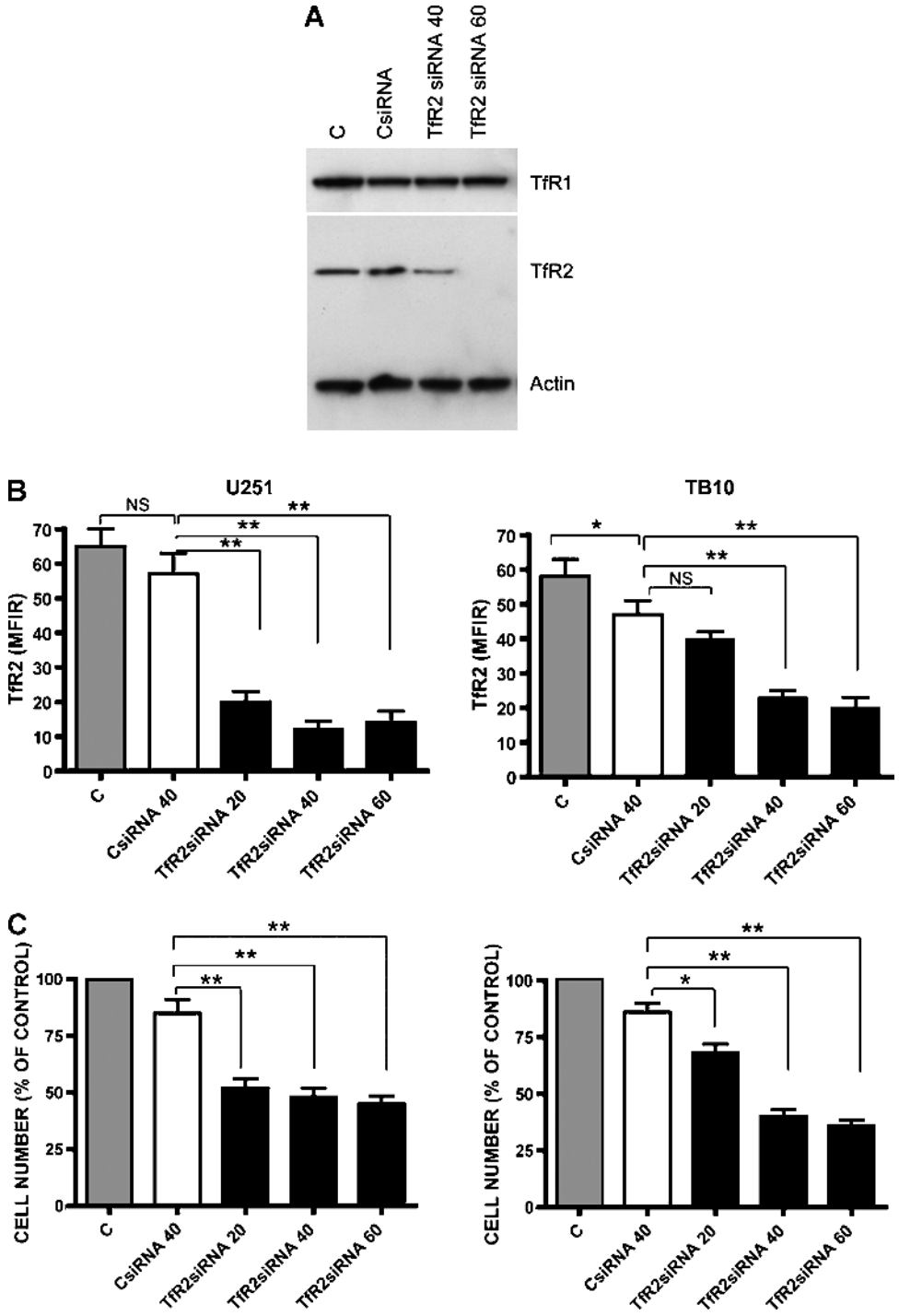

Figure 7. Inhibition of TfR2 expression by siRNA treatment reduces GBM cell growth. (A) Western blot analysis of TfR1 and TfR2 expression in U251 cells transfected with TfR2 siRNA or nontargeting control siRNA (CsiRNA), compared with untreated (C) cells. (B) Flow cytometry analysis of TfR2 expression in U251 and TB10 cells transfected with TfR2 siRNA or CsiRNA. Data represent the mean values ± SEM observed in three independent experiments (*$P < .05$, **$P < .01$; *NS* indicates not significant). (C) After treatment with TfR2, siRNA or CsiRNA U251 and TB10 cells have been analyzed for the number of living cells. Data represent the mean values ± SEM observed in three independent experiments (*$P < .05$, **$P < .01$).

BTSC83 GBM cells do express TfR2 (Figure 8). TfR2 immunoreaction selectively stained the neuroepithelial cells of the tumor xenografts, whereas the stromal component of the xenografts was TfR2-negative.

In line with the positivity of endothelial cells of arterioles and capillaries of primary tumors, we observed also a clear TfR2 positivity at the level of the neoformed blood vessels of GBM xenografts (Figure 9).

Discussion

Glioblastoma multiforme is the most common and aggressive primary malignant brain tumor in adults. Despite improvements in overall survival with the addition of temozolomide to radiation in the adjuvant setting, the prognosis of patients affected by these tumors remains very poor. For these reasons, there is an absolute need for the development

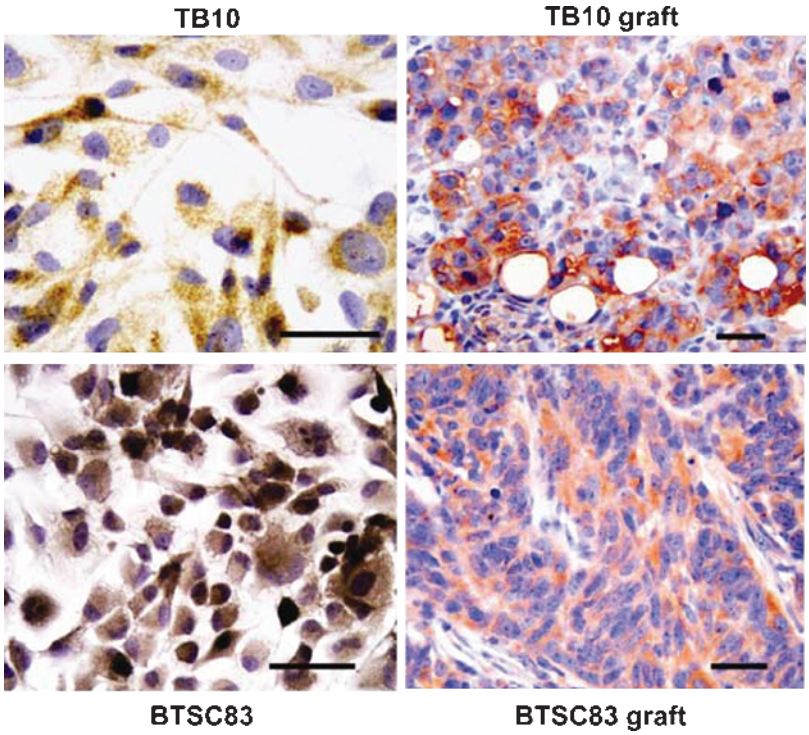

Figure 8. TfR2 expression in GBM xenografts. Tumor xenografts were obtained by subcutaneous injection of either TB10 or BTSC83 human GBM cell lines in nude athymic mice. The tumor xenografts obtained both with TB10 cells and with BTSC83 cells show an intense expression of TfR2 by the tumor cells. Bar, 50 μm.

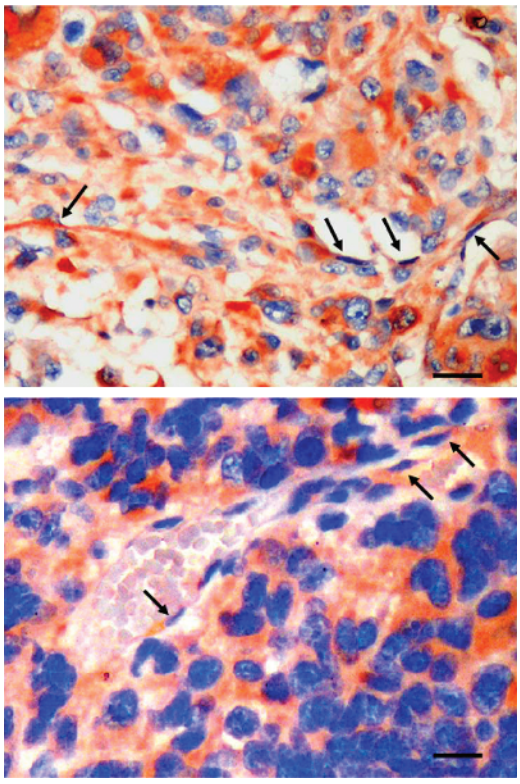

Figure 9. TfR2 expression by the neoformed blood vessels of GBM xenografts. TfR2-positive cells lining the lumen of vascular structures both in TB10 (arrows, upper panel) and in BTSC83 tumor xenografts (arrows, lower panel). Bar, 35 μm.

of innovative therapies. Among them, targeted therapy seems to be particularly challenging. These therapies may target either intracellular signaling pathways (i.e., mammalian target of rapamycin, protein kinase C) or membrane growth factor receptors (i.e., epidermal growth factor receptor or vascular endothelial growth factor receptor). Alternatively, target therapies may be based on the identification of membrane molecules expressed on the surface of glioma cells and not on their normal counterpart.

In this report, we provide evidence for the first time that TfR2 represents a membrane antigen abundantly expressed on malignant glioma cells but not expressed on neural cells as well as on endothelial cells of normal brain. The absence of TfR2 expression in normal brain recently reported by a study showing the absence of TfR2 mRNA in normal human brain, with the exception of cerebellum [30]. In this same study, preliminary evidence about the frequent expression of TfR2 mRNA in human brain tumors, including oligodendroglioma, oligoastrocytoma, and astrocytoma was provided [30]. Our immunohistologic analysis on 81 astrocytic tumors of various histologic grades clearly shows that TfR2 expression is related with malignancy. This finding suggests that the induction of TfR2 in malignant glioma cells may provide a growth advantage to these cells. In line with this interpretation, we observed that in GBM cell lines TfR2 activation induces a rapid and pronounced ERK1/ERK2 phosphorylation. Previous studies have shown that ERK1/ERK2 is constitutively activated in human GBM [31–33] and that the level of ERK1/ERK2 activation represents a negative prognostic factor. In line with this interpretation, we observed that in GBM cells TfR2 appears to be localized at the level of lipid rafts, which are thought to act as molecular sorting mechanisms, capable of coordinating the organization of signal transduction pathways within limited regions of the plasma membrane and organelles [25].

Consistent with this notion, it is tempting to hypothesize that TfR2, which is expressed at high levels on GBM cells, may be constitutively activated by plasmatic holo-Tf. In line with this hypothesis, silencing experiments of TfR2 using TfR2 siRNA showed that TfR2 expression contributes to *in vitro* proliferation of GBM cells. Thus, TfR2 may be continuously involved in ERK1/ERK2 activation, conveying a proliferative/survival signal to cancer cells. Accordingly, previous studies have shown that Ras is very rarely mutated in GBM, suggesting that MAPK-dependent mitogenic signaling in GBM is triggered through inappropriate activation of membrane receptors [34].

We have also observed that the level of TfR2 expression on GBM tumors represents a positive prognostic factor. In fact, patients with high TfR2 expression on their tumor cells survive longer than patients with low TfR2 expression. Because the treatment plan of these patients included radiotherapy and temozolomide [35], we investigated whether GBM cell lines displayed *in vitro* differential sensitivity to temozolomide relative to their TfR2 expression levels. Our results show that $TfR2^+$ GBM cell lines are more sensitive to temozolomide than $TfR2^-$ GBM cell lines. The higher sensitivity of $TfR2^+$ GBM cell lines seems to be associated to TfR2 positivity, but not directly dependent on it, as shown by temozolomide treatment of TfR2 knock down cells. The ensemble of these observations suggests that the expression of TfR2 on GBM tumor cells is associated with a higher sensitivity to the antiproliferative effects of temozolomide and may explain the better prognosis of patients harboring $TfR2^+$ GBM. The finding that the higher sensitivity to temozolomide of $TfR2^+$ cells is associated but not directly linked to TfR2 positivity of the tumor may help to explain why intriguingly TfR2 expression increases with tumor grade but is inversely correlated to patients' survival.

The molecular mechanisms responsible for the induction of TfR2 expression in malignant glioma cells are, at the moment, completely unknown. In normal tissues, TfR2 is expressed only in liver cells and, at lower levels, in epithelial intestinal cells [36]. The mechanisms responsible for the regulation of TfR2 expression at tissue level are also unknown. However, in this context, it is of interest to note that TfR2 gene is located on chromosome 7 at the 7q22 region [5], and this chromosome is very frequently (>75% of cases) involved in numeric chromosomal abnormalities (trisomy/polysomy 7) [37]. Previous studies have shown that various stimuli, including iron levels, nitric oxide, and hypoxia, are able to modulate TfR1 expression in various normal and malignant cells [26,27]. Among these stimuli, it seemed particularly important to evaluate any possible effect of hypoxia on TfR2 expression in GBM cells. It is known that malignant gliomas are among the most vascular of all solid tumors and that hypoxia-dependent pathways are largely involved in the neoangiogenetic mechanisms operating in these tumors [28,38,39]. Particularly, it seemed important to demonstrate that a high TfR2 expression can be maintained even under conditions of hypoxia, which are frequently observed in growing GBM. Our experiments on GBM cell lines showed that $CoCl_2$ and reduced oxygen tension are able to induce an increase of TfR2 expression.

A major finding of our study is that TfR2 is expressed by the stem cell compartment of GBM and that the tumor xenografts generated both by GBM cell lines and by GBM stem cells retain TfR2 expression *in vivo*. These results are of particular interest to design preclinical models of target therapy. In this respect, two features of TfR2 expression on GBM cells seem very suitable for the development of targeted therapy using an immunotoxin based on an anti-TfR2 mAb: 1) TfR2 is clearly expressed on almost all cases of AA and GBM and 2) in most cases, TfR2 is expressed virtually on all tumor cells. Furthermore, the expression pattern of TfR2 seems much more suitable for immunotherapy than that of TfR1. In fact, TfR1 is expressed not only on GBM cells but also on the endothelial cells of the normal brain, whereas TfR2 is expressed only by the tumor cells and not by the normal brain tissue. Pilot clinical trials based on the use of Tf-CRM107, a molecule acting through binding to TfR1, have shown that this conjugate does exert a strong antitumor cytotoxicity and that it also induces a significant peritumoral toxicity owing to thrombosis of cortical vessels [16]. This limiting peritumoral toxicity is not expected using anti-TfR2 immunoconjugates because TfR2 is not expressed on normal brain endothelial cells.

It is of interest to note that we recently described the expression of TfR2 in colon carcinomas (26% of colon carcinomas were $TfR2^+$, whereas normal colon mucosa was TfR^-) [40]. This observation, together with the findings of the present study, indicates that TfR2 is a membrane receptor whose expression in normal tissues is restricted to hepatic cells while it is frequently expressed in tumor cells.

In conclusion, the present study demonstrates for the first time that TfR2 is a tumor neoantigen for human malignant gliomas and that it meets many of the requirements needed to develop target therapies.

Acknowledgments

The authors thank Giuseppe Loreto for help in the preparation of graphs.

Conflict of Interest

The authors declare no conflict of interest.

References

[1] Daniels TR, Delgado T, Rodriguez JA, Helguera G, and Penichet ML (2006). The transferrin receptor, part I: Biology and targeting with cytotoxic antibodies for the treatment of cancer. *Clin Immunol* **121**, 144–158.

[2] Kawabata H, Yang R, Hirama T, Vuong PT, Kawano S, Gombart AF, and Koeffler HP (1999). Molecular cloning of transferrin receptor 2: a new member of the transferrin receptor-like family. *J Biol Chem* **274**, 20826–20832.

[3] Kawabata H, Nakamaki T, Ikonomi P, Smith RD, Germani RS, and Koeffler HP (2001). Expression of transferrin receptor 2 in normal and neoplastic hematopoietic cells. *Blood* **98**, 2714–2719.

[4] Fleming RE, Migas MC, Holden CC, Waheed A, Britton RS, Tomatsu S, Bacon BR, and Sly W (2000). Transferrin receptor 2: continued expression in mouse liver in the face of iron overload and in hereditary hemochromatosis. *Proc Natl Acad Sci USA* **97**, 2214–2219.

[5] Camaschella C, Roetto A, Cali A, De Gobbi M, Gorozzo G, Carella M, Majorano N, Totaro A, and Gasparini P (2000). The gene *TFR2* is mutated in a new type of haemochromatosis mapping to 7q22. *Nat Genet* **25**, 14–15.

[6] Roetto A, Totaro A, Piperno A, Piga A, Longo F, Garozzo G, Calì A, De Gobbi M, Gasparini P, and Camaschella C (2001). New mutations inactivating transferrin receptor 2 in hemochromatosis type 3. *Blood* **97**, 2555–2560.

[7] Calzolari A, Raggi C, Deaglio S, Sposi NM, Stafsnes M, Fecchi K, Parolini I, Malavasi F, Peschle C, Sargiacomo M, et al. (2006). TfR2 localizes in lipid raft domains and is released in exosomes to activate signal transduction along the MAPK pathway. *J Cell Sci* **119**, 4486–4498.

[8] Calzolari A, Oliviero I, Deaglio S, Mariani G, Biffoni M, Sposi NM, Malavasi F, Peschle C, and Testa U (2007). Transferrin receptor 2 is frequently expressed in cancer cell lines. *Blood Cells Mol Dis* **39**, 82–91.

[9] McCarthy BJ and Kruchko C (2005). Consensus conference on cancer registration of brain and central nervous system tumors. *Neuro Oncol* **7**, 196–201.

[10] Hegi ME, Diserens AC, Gorlia T, Hamou MF, De Tribolet N, Weller M, Kros JM, Henfellner JA, Maosn W, Mariani L, et al. (2005). MGMT gene silencing and benefit from temozolomide in glioblastoma. *N Engl J Med* **352**, 997–1003.

[11] Demuth T and Berens ME (2004). Molecular mechanisms of glioma cell migration and invasion. *J Neuroncol* **70**, 217–228.

[12] Recht L, Torres CO, Smith TW, Raso V, and Griffin TW (1990). Transferrin receptor in normal and neoplastic brain tissue: implications for brain-tumor immunotherapy. *J Neurosurg* **72**, 941–945.

[13] Hall WA, Godal A, Juell S, and Fodstad O (1992). *In vitro* efficacy of transferrin-toxin conjugates against glioblastoma multiforme. *J Neurosurg* **76**, 838–844.

[14] Chirasani SR, Markovic DS, Synowitz M, Eichler SA, Wisniewski P, Kamiska B, Otto A, Wanker E, Schafer M, Chiarugi P, et al. (2008). Transferrin-receptor–mediated iron accumulation controls proliferation and glutamate release in glioma cells. *J Mol Med* **87**, 153–167.

[15] Richardson DR (2002). Iron chelators as therapeutic agents for the treatment of cancer. *Crit Rev Oncol Hematol* **42**, 267–281.

[16] Laske DW, Youle RJ, and Oldfield EH (1997). Tumor regression with regional distribution of the targeted toxin TF-CRM107 in patients with malignant brain tumors. *Nat Med* **3**, 1362–1368.

[17] Weaver M and Laske DW (2003). Transferrin receptor ligand–targeted toxin conjugate (Tf-CRM107) for therapy of malignant gliomas. *J Neurooncol* **65**, 3–13.

[18] Deaglio S, Capobianco A, Cali A, Bellora F, Alberti F, Righi L, Sapino A, Camaschella C, and Malavasi F (2002). Structural, functional, and tissue distribution analysis of human transferrin receptor-2 by murine monoclonal antibodies and a polyclonal antiserum. *Blood* **100**, 3782–3789.

[19] Ricci-Vitiani L, Larocca LM, Lombardi DG, Signore M, Pierconti F, Petrucci G, Montano N, Maira G, and De Maria R (2008). Mesenchymal differentiation of glioblastoma stem cells. *Cell Death Diff* **9**, 1491–1498.

[20] Lisanti MP, Tang ZL, and Sargiacomo M (1993). Caveolin forms a hetero-oligomeric protein complex that interacts with an apical GPI-linked protein: implications for the biogenesis of caveolae. *J Cell Biol* **123**, 595–604.

[21] Parolini I, Sargiacomo M, Lisanti MP, and Peschle C (1996). Signal transduction and glycophosphatidylinositol-linked proteins (lyn, lck, CD4, CD45, G proteins, and CD55) selectively localize in Triton-insoluble plasma membrane domains of human leukemic cell lines and normal granulocytes. *Blood* **87**, 3783–3794.

[22] Burger PC and Scheithauer BW (1993). Atlas of Tumor Pathology. *Tumors of the Central Nervous System* Vol. 10. Washington, DC: Armed Forces Institute of Pathology, 4–7.

[23] Falchetti ML, Pierconti F, Casalbore P, Maggiano N, Levi A, Larocca LM, and Pallini R (2003). Glioblastoma induces vascular endothelial cells to express telomerase *in vitro*. *Cancer Res* **63**, 3750–3754.

[24] Eramo A, Ricci-Vitiani L, Zeuner A, Pallini R, Lotti F, Sette G, Pilozzi E, Larocca LM, Peschle C, and De Maria R (2006). Chemotherapy resistance of glioblastoma stem cells. *Cell Death Diff* **13**, 1238–1241.

[25] Simons K and Toomre D (2000). Lipid rafts and signal transduction. *Nat Rev Mol Cell Biol* **1**, 31–39.

[26] Tacchini L, Bianchi L, Bernelli-Zazzera A, and Cairo G (1999). Transferrin receptor induction by hypoxia. *J Biol Chem* **274**, 24142–24146.

[27] Toth I, Yuan L, Rogers JT, Boyce H, and Bridges KR (1999). Hypoxia alters iron-regulatory protein-1 binding capacity and modulates cellular iron homeostasis in human hepatoma and erythroleukemia cells. *J Biol Chem* **274**, 4467–4473.

[28] Jain RK, Di Tomaso E, Duda DG, Loeffler JS, Sorensen AG, and Batchelor TT (2007). Angiogenesis in brain tumours. *Nat Rev Neurosci* **8**, 610–622.

[29] Pallini R, Sorrentino A, Pierconti F, Maggiano N, Faggi R, and Montano N (2006). Telomerase inhibition by stable RNA interference impairs tumor growth and angiogenesis in glioblastoma xenografts. *Int J Cancer* **118**, 2158–2167.

[30] Hanninen MM, Haapasalo J, Haapasalo H, Fleming RE, Britton RS, Bacon BR, and Parkkila S (2009). Expression of iron-related genes in human brain and brain tumors. *BMC Neurosci* **10**, 1–9.

[31] Bhaskara VK, Panigrahi M, Challa S, and Babu PP (2005). Comparative status of activated ERK1/2 and PARP cleavage in human gliomas. *Neuropathology* **25**, 48–53.

[32] Lama G, Mangiola A, Anile C, Sabatino G, De Bonis P, Lauriola L, Giannitelli C, La Torre G, Jhanwar-Uniyal M, Sica G, et al. (2007). Activated ERK1/2 expression in glioblastoma multiforme and in peritumor tissue. *Int J Oncol* **30**, 1333–1342.

[33] Mangiola A, Lama G, Giannitelli C, De Bonis P, Anile C, Lauriola L, La Torre G, Sabatino G, Maira G, Jhanwar-Uniyal M, et al. (2007). Stem cell marker nestin and c-Jun NH_2-terminal kinases in tumor and peritumor areas of glioblastoma multiforme: possible prognostic implications. *Clin Cancer Res* **13**, 6970–6977.

[34] Furnari FB, Fenton T, Bachoo RM, Mukasa A, Stommel JM, Stegh A, Hahn WC, Ligon KL, Louis DN, Brennan C, et al. (2007). Malignant astrocytic glioma: genetics, biology, and paths to treatment. *Genes Dev* **21**, 2683–2710.

[35] Pallini R, Ricci-Vitani L, Banna GL, Signore M, Lombardi D, Todaro M, Stassi G, Martini M, Maira G, Larocca LM, et al. (2008). Cancer stem cell analysis and clinical out come in patients with glioblastoma multiforme. *Clin Cancer Res* **14**, 8205–8212.

[36] Calzolari A, Oliviero I, and Testa U (2007). Transferrin receptor 2 is emerging as a major player in the control of iron metabolism. *Cent Eur J Biol* **2**, 34–55.

[37] Lopez-Gines C, Cerda-Nicolas M, Gil-Benso R, Pellin A, Lopez-Guerrero JA, Callaghan R, Benito R, Roldan P, Piquer J, Llacer J, et al. (2005). Association of chromosome 7, chromosome 10 and EGFR gene amplification in glioblastoma multiforme. *Clin Neuropathol* **24**, 209–218.

[38] Fukumura D, Xu L, Chen Y, Gohongi T, Seed B, and Jain RK (2001). Hypoxia and acidosis independently up-regulate vascular endothelial growth factor transcription in brain tumors *in vivo*. *Cancer Res* **61**, 6020–6024.

[39] Helmlinger G, Yuan F, Dellian M, and Jain RK (1997). Interstitial pH and Po_2 gradients in solid tumors *in vivo*: high-resolution measurements reveal a lack of correlation. *Nat Med* **3**, 177–182.

[40] Calzolari A, Deaglio S, Maldi E, Cassoni P, Malavasi F, and Testa U (2009). TfR2 expression in human colon carcinomas. *Blood Cells Mol Dis* **43**, 243–249.